Journal of Information Processing Systems, Vol.6, No.3, September 2010 DOI : 10.3745/JIPS.2010.6.3.347

A Measurement System for 3D Hand-Drawn Gesture with a PHANToM™ Device

Seong Young Ko*, Won-Chul Bang** and Sang-Youn Kim***

Abstract—This paper presents a measurement system for 3D hand-drawn gesture motion. Many pen-type input devices with Inertial Measurement Units (IMU) have been developed to estimate 3D hand-drawn gesture using the measured acceleration and/or the angular velocity of the device. The crucial procedure in developing these devices is to measure and to analyze their motion or trajectory. In order to verify the trajectory estimated by an IMU-based input device, it is necessary to compare the estimated trajectory to the real trajectory. For measuring the real trajectory of the pen-type device, a PHANToMTM haptic device is utilized because it allows us to measure the 3D motion of the object in real-time. Even though the PHANToMTM measures the position of the hand gesture well, poor initialization may produce a large amount of error. Therefore, this paper proposes a calibration method which can minimize measurement errors.

Keywords—Hand-Drawn Gesture, Hand-Held Device, Inertial Measurement Unit, PHANToM™, Calibration

1. INTRODUCTION

Recently, hand-held devices have become very popular and have become an important part of our life. People communicate with each other and send messages using their hand-held devices. They also play games, listen to music, and watch TV or movies using their hand-held devices. To select the menus on the hand-held devices, people usually use a keypad or a touch screen. Recent technological advancement in hardware and software has reached the point where the user does not need to press or touch the keypad or the screen. Speech recognition [1] and vision-based gesture recognition devices [2] are good examples of touch less interaction. Although these systems have great potential for hand-held devices, they are not yet widely used due to performance degradation in noisy environments and changing lighting conditions. One way of resolving the aforementioned issues is to develop pen-type devices that can be used for various input commands and that can digitize the trajectory of writing or drawing. Some of these endeavors have been commercialized and publicized in the form of patents and papers. One of the

※ This research was supported by the Converging Research Center Program through the National Research Foundation of Korea (NRF) funded by the Ministry of Education, Science and Technology (2009-0082271). This work was partly supported by the IT R&D program of MKE/KEIT [KI001824, Development of Digital Guardian technology for the disabled and the aged person].

Manuscript received June 9, 2010; accepted August 27, 2010.

Corresponding Author: Sang-Youn Kim

* Mechatronic in Medicine Lab., Imperial College London, United Kingdom

** Samsung Advanced Institute of Technology (SAIT), Korea

*** Interaction Lab., Advanced Technology Research Center, Korea University of Technology and Education, Korea (sykim@kut.ac.kr)

most popular devices is a 'Wacom tablet' with a digitizer pen, which uses electromagnetic resonance technology [3]. Since the tablet transmits power to the digitizer pen through resonant coupling, no batteries are required for the pen. However, the digitizer pen is not self-contained for it only works on the tablet. Zloter and Shenholz used a wireless transceiver chip that can communicate with a pen-type device [4]. In this technology, the position of the pen's tip is computed by the triangulation method using an ultrasonic signal synchronized with an infrared signal, which is generated by the chip that can be positioned on any notepad using a clip-shaped connector. However, this ultrasonic and infrared pen-type device also has a disadvantage in that it can work only with a nearby infrared chip. Another method of commercialized technology is based on pattern recognition by a small camera embedded into the pen's tip. The coded patterns on a paper are captured by the camera and interpreted to localize the absolute coordinates of the tip on the paper [5]. Several pen-shaped optical mice have been also commercialized to digitize the trajectory of one's writing. Since the lying angle (or tilting angle) between the pen and the writing surface is not constant, it is not easy to detect the movement exactly. Thus, these systems require a robust structure to reliably capture the reflected light of light-emitting diodes (LEDs) in workspace [6]. These pen-type devices are self-contained but can only detect the trajectory while the devices are touching the writing surface, resulting in only partial reconstruction of handwriting trajectory. In order to develop intrinsically self-contained hand-held devices, the inertial sensors such as accelerometers and/or gyroscopes are integrated to the system [7-10]. The trajectory can be computed by integrating the sensor signals but the numerical integration results in a drift error which grows as a function of time.

To accurately obtain the trajectory of writing/drawing, a self-contained digital pen system consisting of inertial sensors and an optical sensor was developed [11]. In order to investigate the trajectory estimated by an inertial measurement unit (IMU) and to compute its error according to the various trajectory expectation algorithms, it is necessary to measure the real trajectory of the pen-type input device. Although motion capture systems or vision systems were commonly used to measure hand motion in 3-dimensional space, the measurement system consisting of mechanical links is believed to be more reliable and robust with minimizing errors. In our study, we have used a PHANToM™ haptic device to measure the trajectory of a pen-type device in real-time. Even though the PHANToM™ device measures the position of hand gesture well with high repeatability, poor initialization may produce a large amount of error. Therefore, in this paper, we calibrated the PHANToM™ device and constructed a measurement system that acquires the trajectory of the pen-type device.

This paper is organized as follows. Section 2 describes the developed hand-held device and the measurement system. Section 3 presents simple and preliminary testes to verify the measurement system. Section 4 illustrates the calibration method to improve its accuracy. Finally, in Section 5, a summary of the presented work and the direction of our future research are described.

2. SYSTEM STRUCTURE

There are several issues in combining these two sensing principles. First, the dimensional scale and the coordinates from two sensors are not identical. Second, the qualities of their trajectories depend on the pen's states (whether the pen touches the writing surface or not) and the time interval of integral calculus. The first problem is rather simple to solve. The optical sensor

at the pen-tip measures incremental movements in both horizontal and vertical directions while the IMU measures the spatial position. To align these measurements in the same scale and the same coordinate, we need to transform the pen-down trajectory measured in the optical coordinate to that of the inertial coordinate. Although the inertia-based dead reckoning can provide a solution, dead reckoning has a critical limitation as its errors are accumulated and its accuracy is severely lessened if the time interval is too long. In this work, we assumed that the users write characters without any hesitation and the pen's state (from pen-up to pen-down, and vice versa) changes quickly. Therefore, the duration between strokes (pen-up state) can be assumed to be less than a second. Under this assumption, we could enhance the accuracy of trajectory estimation by comparing the optics-based and the inertia-based trajectories during the pen-down states and the pen-up states.

Fig. 1 shows the overall block diagram. We used an optical sensor (1) to obtain x and y position in the optical coordinate (2). An inertial sensor was applied to our system for obtaining x, y, and z position by double integration of acceleration after gravity removal and coordinate transformation in the inertial coordinate (5). By comparing the two trajectories during the pen-down state (3), the relationship between two coordinates with different length scales can be obtained. The role of the block (3) is to transform the pen-down trajectory measured in the optical coordinate into the trajectory measured in the inertial coordinate. Another role of the block (3) is to establish the drift model for offsets which can appear while utilizing a tri-axis accelerometer and three single-axis gyroscopes. We have to compute the drift error with the drift model in real-time because the drift in the offset slowly varies over time (6). Usually, the amount of the drift of an accelerometer and a gyroscope can be modeled as a constant for a short period, e.g. a few seconds. The drift model established at the previous pen-down state is used to compensate for the current inertia-based pen-up trajectory (7)-(8). The pen-down trajectory and the pen-up trajectory in the same coordinate now can be combined to present the complete handwriting cycle(9).

A PHANToM^{TM} haptic (Premium 1.0) device was used to measure the real 3D trajectory of the used pen-type input device. The PHANToM^{TM} is a mechanical device that is specifically used for providing haptic feedback to a user. The device can measure the motion of its end-effector or its handle, and can produce feedback force when a user interacts with a virtual or real object. In our work, we used the device as a measurement tool to evaluate trajectory obtained from the pen-type input device (real-trajectory). The pen-type device was attached to the gimbal

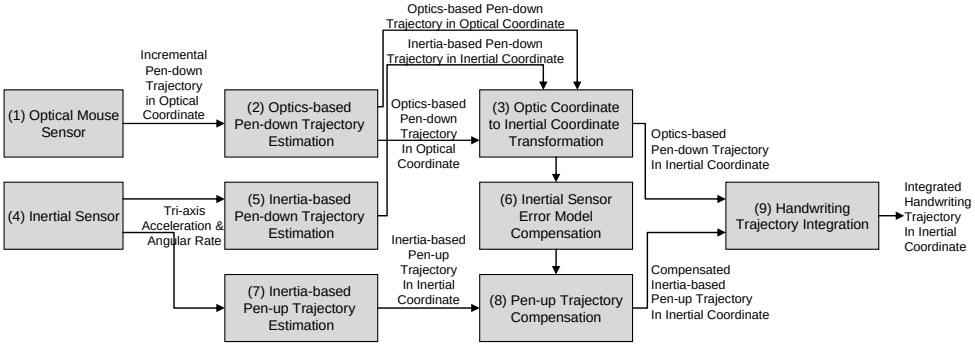

Fig. 1. Overall procedure in trajectory estimation

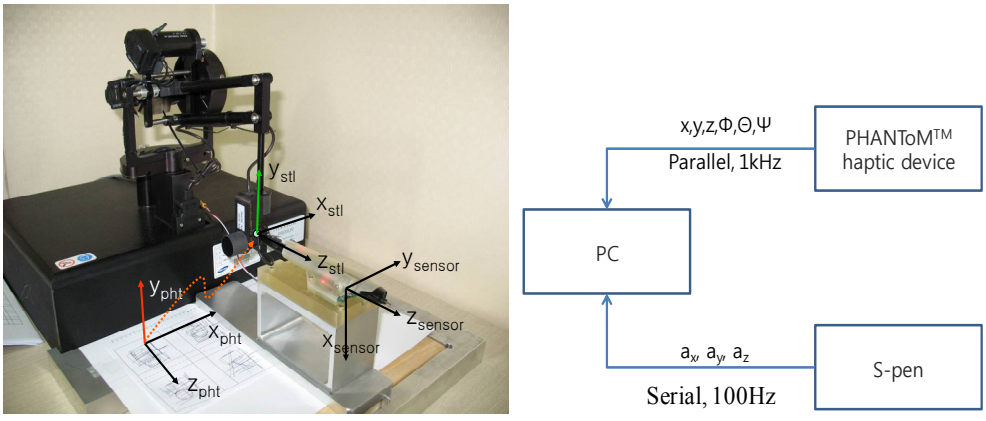

Fig. 2. Hardware configuration (a) and software structure (b)

of the PHANToM™ to measure the trajectories at the same time. Fig. 2(a) shows the hardware configuration for measuring the two trajectories. In this system, the pen-type device and the PHANToM™ device were connected to the same PC via serial and parallel port, respectively as shown in Fig 2(b). The hand motion (x, y, z, Φ, θ, Ψ) was obtained from the haptic device at 1kHz and the acceleration values (ax, ay, az) were also acquired from the pen-type device at 100Hz.

3. Preliminary Tests for System Verification

A series of preliminary tests was performed to verify the proposed measurement system. In the preliminary tests, subjects wrote characters with the pen-type input device that is attached to the gimbal of the PHANToM™. Since the PHANToM™ device is proven to have high positional accuracy [13], we focused on the comparison of data from the PHANToM™ device and the pen-type device.

3.1 Comparison of Accelerations Measured by PHANToM™ and a Pen-type Input Device

To precisely compare the trajectory of the PHANToM™ and that of the pen-type input device, it is necessary to compute both trajectories in the same coordinate system. Three coordinate systems (PHANToM™ coordinate, stylus coordinate, and sensor coordinate) were considered as shown in Fig. 2(a). The PHANToM™ coordinate was defined as the fixed coordinate system located at the initial position of the stylus coordinate system and it was considered the world coordinate system. The stylus coordinate system was attached to the stylus. With regard to the sensor coordinate system, it was attached to the acceleration sensor in the pen-type input device. The position of the sensor mounted on the pen-type device in the PHANToM™ coordinate system (${}^{pht}P_{sensor}$) can be calculated through equation (1). The transformation matrix (${}^{pht}T_{stl}$) from the

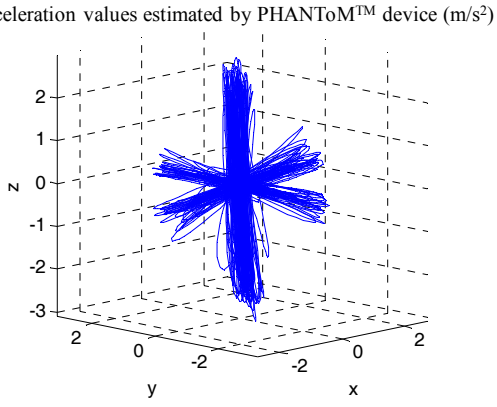

Fig. 3. Measured acceleration of the tip of the stylus

PHANToM™ coordinate system to the stylus coordinate system can be obtained from the OpenHaptics Library. The origin of the sensor coordinate ($^{stl}P_{sensor}$) in the stylus coordinate system was designed to be [1.9, -6.5, 121.9] mm. A series of low pass filters (τ =0.07 sec) were used to smoothen the output signal. Fig. 3 shows the acceleration values obtained by equation (1) while shaking the PHANToM™ stylus in the x, y and z directions, sequentially.

$$\begin{bmatrix} {}^{pht}P_{sensor} \\ 1 \end{bmatrix} = {}^{pht}T_{stl} \times \begin{bmatrix} {}^{stl}P_{sensor} \\ 1 \end{bmatrix} = \begin{bmatrix} {}^{pht}R_{stl} & {}^{pht}P_{stl} \\ [0,0,0] & 1 \end{bmatrix} \times \begin{bmatrix} {}^{stl}P_{sensor} \\ 1 \end{bmatrix} \quad (1)$$

where, ${}^{pht}P_{sensor} \in \mathrm{R}^3$, ${}^{stl}P_{sensor} \in \mathrm{R}^3$, ${}^{pht}P_{stl} \in \mathrm{R}^3$, ${}^{pht}T_{stl}$ is 4 x 4 matrix, ${}^{pht}R_{stl}$ is 3 x 3 matrix.

As the next step, we compared the acceleration value measured by PHANToM™ with the acceleration value obtained by the pen-type input device. We shook the pen-type device in the following directions (Fig. 4 : y_{pht} (①), x_{pht}(②), z_{pht}(③), x_{pht}(④), y_{pht}(⑤), and z_{pht}(⑥). After that, we moved it in order for the direction of the z_{sensor} heads for $[1,1,1]^T$ in the PHANToM™ to coordinate and then shook it again in the following directions: z_{sensor}(⑦), y_{pht}(⑧), x_{pht}(⑨), and z_{pht}(⑩). The acceleration values measured by different methods should be identical considering the coordinate system with which the values are expressed. As shown in Fig. 2(a), x_{pht}, y_{pht} and z_{pht} are parallel to y_{sensor}, $-x_{sensor}$ and z_{sensor} in the initial state, respectively. Therefore, when the stylus is being shaken in y_{pht} direction as indicated by ① in Fig. 4, the acceleration of the tip should be along y_{pht}, and at the same time it should be measured along $-x_{sensor}$. As shown in Fig. 4, the y-component of the acceleration values (Phantom y) in the PHANToM™ coordinate are reversely parallel with the x-component of acceleration values (Pen x) in the sensor coordinate. In the same way, the acceleration values along *Phantom x* and *Phantom z* are parallel with the values along *Pen y* and *Pen z*, respectively. Please note that the offsets (about 9.8m/sec^2) in Pen x, Pen y and Pen z are presented due to the gravity according to the pen's posture.

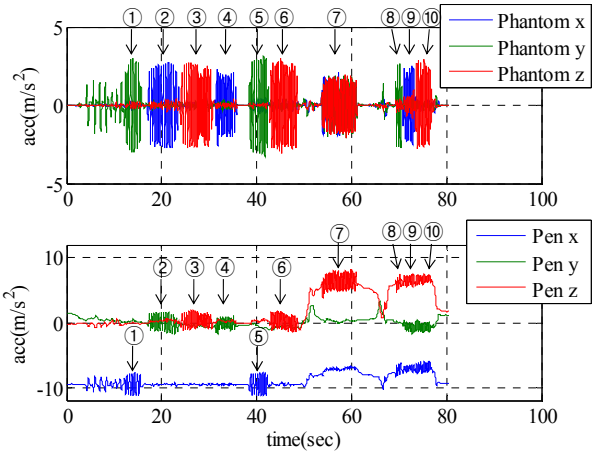

Fig. 4. Comparison of accelerations by the PHANToM™ and the pen-type device

3.2 Comparison of Accelerations Measured by PHANToM™ and a Pen-type Input Device

In this section, we discuss how to express the posture of the pen-type input device by the Euler angles. We utilized the Z-Y-X Euler angle definition [14] as shown in equation (2). In the Z-Y-X Euler angle definition, the movable coordinate, which can be considered the sensor coordinate, is rotated ψ radian about its z-axis, then θ radian about the moved y-axis, and finally φ radian about the moved x-axis.

$$
\begin{aligned}
R &= R_z(\psi)R_y(\theta)R_x(\phi) \\
&= \begin{bmatrix} c\psi & -s\psi & 0 \\ s\psi & c\psi & 0 \\ 0 & 0 & 1 \end{bmatrix}\begin{bmatrix} c\theta & 0 & s\theta \\ 0 & 1 & 0 \\ -s\theta & 0 & c\theta \end{bmatrix}\begin{bmatrix} 1 & 0 & 0 \\ 0 & c\phi & -s\phi \\ 0 & s\phi & c\phi \end{bmatrix} \\
&= \begin{bmatrix} c\psi\, c\theta & c\psi\, s\theta\, s\phi - s\psi\, c\phi & c\psi\, s\theta\, c\phi + s\psi\, s\phi \\ s\psi\, c\theta & s\psi\, s\theta\, s\phi + c\psi\, c\phi & s\psi\, s\theta\, c\phi - c\psi\, s\phi \\ -s\theta & -c\theta\, s\phi & c\theta\, c\phi \end{bmatrix}
\end{aligned}
\tag{2}
$$

where,

$R_x(\varphi)$: rotation matrix for rotation φ about x-axis,
$R_y(\theta)$: rotation matrix for rotation θ about y-axis,
$R_z(\psi)$: rotation matrix for rotation ψ about z-axis,
c ψ, s ψ: cos(ψ) and sin(ψ), respectively,
c θ, s θ: cos(θ) and sin(θ), respectively,
c φ, s φ: cos(φ) and sin(φ), respectively.

$$R_{comp} = \begin{bmatrix} 0 & -1 & 0 \\ 1 & 0 & 0 \\ 0 & 0 & 1 \end{bmatrix} \tag{3}$$

$$\begin{aligned} {}^{pht}R_{sensor} &= R_z(\psi)R_y(\theta)R_x(\phi)R_{comp} \\ &= \begin{bmatrix} c\psi\, s\theta\, s\phi - s\psi\, c\phi & -c\psi\, c\theta & c\psi\, s\theta\, c\phi + s\psi\, s\phi \\ s\psi\, s\theta\, s\phi + c\psi\, c\phi & -s\psi\, c\theta & s\psi\, s\theta\, c\phi - c\psi\, s\phi \\ c\theta\, s\phi & s\theta & c\theta\, c\phi \end{bmatrix} \\ &= \begin{bmatrix} R_{00} & R_{01} & R_{02} \\ R_{10} & R_{11} & R_{12} \\ R_{20} & R_{21} & R_{22} \end{bmatrix} \end{aligned} \tag{4}$$

In case of our configuration (Fig. 2(a)), since the initial coordinate system of the pen-type input device was rotated -90 degrees about the z_{pht} axis of the PHANToM^{TM} coordinate, we used the compensation matrix (equation (3)). Therefore, the final transformation matrix (${}^{pht}R_{sensor}$) from the PHANToM^{TM} coordinate system to the sensor coordinate system can be expressed as an equation (4). We can obtain three rotational angles through simple calculation (equation (5)). This equation produces two solutions, both of which are true solutions. In our study, it was assumed that the value of cosθ at the writing posture is positive.

$$\begin{aligned} \phi &= \text{atan2}(\pm R_{20}, \pm R_{22}) \\ \theta &= \text{atan2}(\text{R}_{21}, \pm\sqrt{\text{R}_{20}^2 + \text{R}_{22}^2}) \\ \psi &= \text{atan2}(\mp R_{11}, \mp R_{01}) \end{aligned} \tag{5}$$

Through equation (5), we can obtain the posture of the pen-type input device. In order to verify these calculated posture angles, we measured and displayed the raw acceleration values of the sensor and the calculated angles as shown in Fig. 5 and Table 1. By observing the measured

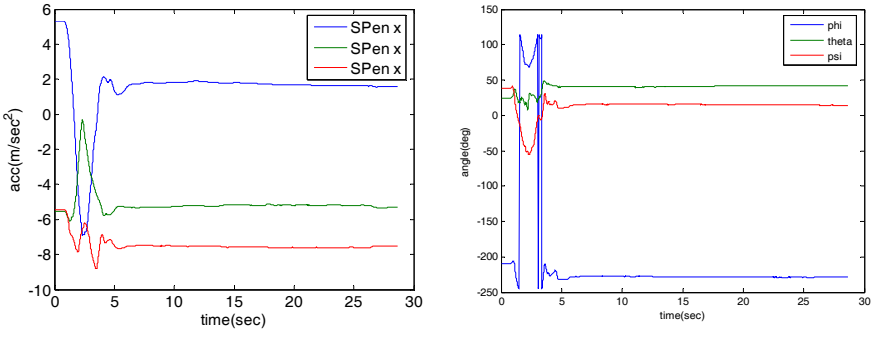

(a) Measured acceleration values (b) Calculated rotational angles

Fig. 5. Typical acceleration and computed angles during writing

Table 1. Average acceleration values and Euler angles during 10sec to 25sec

Situation	Time (sec)	Approximated Acceleration Value (m/s^2)	Approximated Measured Angle (degrees)
Writing posture	10~25	[1.7, -5.2, -7.6]	$[\Phi,\theta,\Psi] = [131, 41, 15]$

acceleration values which are caused by the gravity in the direction of the negative z-axis, we can estimate the posture of the pen-type input device. Please note that the period from 0 sec to 5 sec should be ignored because the pen was moving during this period.

The posture of the pen-type input device is very similar to normal writing posture if the sensor coordinate system is rotated 15 degrees about the z -axis, then 41 degrees along the moved y-axis of the sensor coordinate system, 131 degrees about the moved x-axis of the sensor coordinate, and finally 90 degrees along the moved z-axis. In the posture of the pen-type input device, the initial configuration of the sensor coordinate system is identical to that of the PHANToM™ coordinate system. The last rotation indicates the compensation matrix explained in equation (3). Therefore we could say that the measured rotational angles are quite reasonable.

4. CALIBRATIONS

Accuracy and repeatability of the PHANToM™ are sufficient to measure the accurate position of a target object due to its high-resolution encoders. The PHANToM™ is initialized in the powered-on position. To minimize initialization error caused by initial posture, we need to turn on the power of the PHANToM™ at a specific location where the user's guide recommends. For this purpose, we designed mechanical interfaces, one of which connects the pen-type device to the gimbal of the PHANToM™ device, and the other of which fixes the position of the aforementioned connector at a specific location from the base of the PHANToM™ device, as shown in Fig. 2. However, a joint angles' offset can be present due to the manufacturing error of the mechanical calibration device and the assembly error between the PHANToM™ system and the pen-type device.

For eliminating these offset values, we first attached a calibration paper on the writing plane as shown in Fig. 6(a). We marked nine points of known distance on the calibration paper with the tip of the pen-type device, which is attached to the gimbal of the PHANToM™. Four different postures were measured at each marked point, and this procedure was repeated at five different heights. Through these procedures, we could obtain 180(9x4x5) pairs of the desired tip positions and measured joint angles. Fig. 6(b) and Fig. 6(c) show the desired tip points and the tip points calculated by the measured joint angles before calibration.

In order to calibrate the overall measuring system, we assumed that deviations are mainly from poor initial position of the PHANToM™'s six joints. We also assumed that there are three translational deviations accumulated during the assembly of the pen-type device to the PHANToM™'s stylus. Since the PHANToM™'s last joint deviation is directly related to the translational deviation of assembly, we can eliminate this error parameter by assuming that the joint's error is solely coming from connecting the pen-type device. Therefore, the total number of the deviations to be calibrated becomes eight as shown equation (6). In equation (6), $\Delta\theta_{1st}$, $\Delta\theta_{2nd}$, $\Delta\theta_{3rd}$, $\Delta\theta_{4th}$, and $\Delta\theta_{5th}$ indicate the set of joints' deviations in the PHANToM™ device, and Δx, Δy, and Δz indicate those of the assembly.

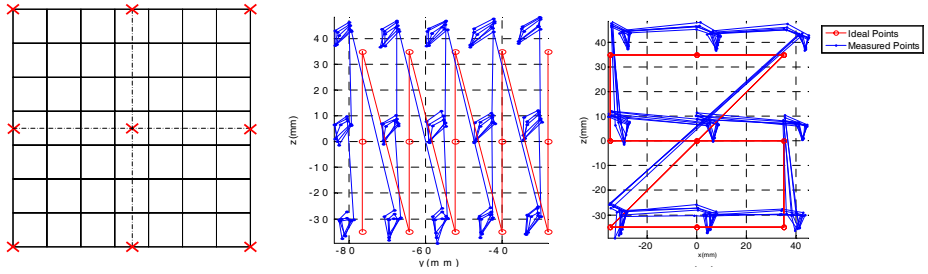

(a) the conceptual diagram of the calibration paper

(b) y-z plane view of ideal points and measured points

(c) x-z plane view of ideal points and measured points

Fig. 6. Results before calibration

$$d = \begin{bmatrix} \Delta\theta_{1st} & \Delta\theta_{2nd} & \Delta\theta_{3rd} & \Delta\theta_{4th} & \Delta\theta_{5th} & 0 & \Delta x & \Delta y & \Delta z \end{bmatrix} \tag{6}$$

In this study, calibration was defined as the procedure to find the set of deviations that minimizes the sum of errors between the desired and measured points. In other words, the calibration is to minimize the cost function ξ_d using equations (7-9).

$$d_{calib} = \arg\min_{D}(\xi_d) \tag{7}$$

$$\xi_d = \sum_{i=1}^{n} \left| P_{des,i} - P_{calc,i}(d) \right|, \quad where \;\; n = 180 \tag{8}$$

$$P_{calc,i}(d) = P_{calc,i}([\Delta\Theta, \Delta T]) = K_{forward}(\Theta_{mea,i} + \Delta\Theta) + \Delta T \tag{9}$$

where,

$$\Theta_{mea,i} = [\theta_{1,i} \cdots \theta_{6,i}], \quad \Delta\Theta = [\Delta\theta_1 \cdots \Delta\theta_5, 0], \quad \Delta T = [\Delta x, \Delta y, \Delta z]$$

d: possible sets of deviations,
$P_{des,i}$: the i^{th} desired point,
$P_{calc,i}(d)$: the i^{th} measured point that is calculated using the measured joint angles and the set of the deviations,
$K_{forward}(\Theta)$: the forward kinematics of the PHANToM^{TM} device.

The calibrated sets of deviations of the joints d_{calib} were obtained by local minimum searching and random searching. We summarized the results in Table 2. To obtain the calibrated tip position, $\Delta\Theta$ was applied to the configuration software, provided by SensAble technology, and ΔT was also applied to our custom software using equation (10). Fig. 7 shows the desired points and measured points after the calibration. We compared the distance errors between the desired and measured tip points before and after the calibration (Table 3).

Table 2. The results of calibration

Sum of Distance (mm)	Average Distance (mm)	Deviation Values	
		$[\theta_{1st} \quad \theta_{2nd} \quad \theta_{3rd} \quad \theta_{4th} \quad \theta_{5th} \quad 0]$ (rad)	$[\Delta x \quad \Delta y \quad \Delta z]$ (mm)
		[0.0017, -0.0130, 0.0092, 0.0517, -0.0488, 0]	[-3.79, 1.78, -3.52]

Table 3. Comparisons of the distance errors before and after calibration

	Sum of Distance Errors (mm, 72 points)	Average Distance Errors (mm)	Standard Deviation of the Error (mm)
Before Calibration	701.8	9.75	2.11
After Calibration	90.9	1.26	0.73

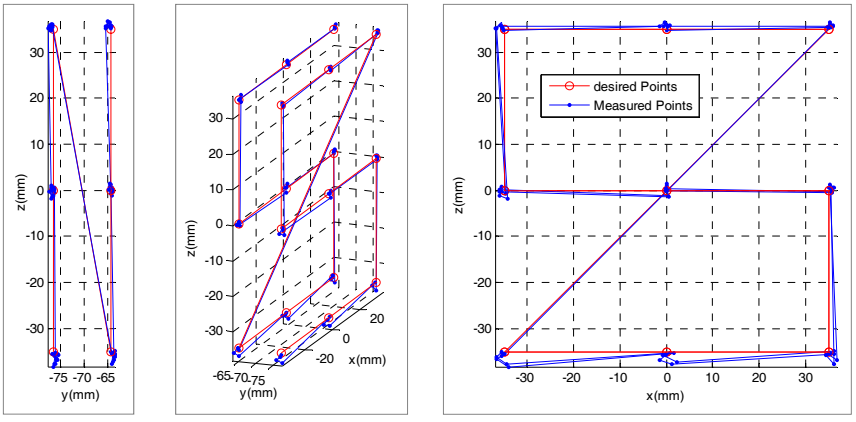

(a) Side view (b) Arbitrary view (c) Top view

Fig. 7. The desired and measured points after calibration

$$\begin{bmatrix} {}^{pht}P_{tip} \\ 1 \end{bmatrix} = {}^{pht}Tr_{stl} \times \begin{bmatrix} {}^{stl}P_{tip} + \Delta T \\ 1 \end{bmatrix} \tag{10}$$

where, ${}^{pht}P_{tip} \in \mathrm{R}^3$, ${}^{stl}P_{tip} \in \mathrm{R}^3$, and ${}^{pht}Tr_{stl}$ is 4 x 4 matrix

5. CONCLUSION

This paper focuses on presenting a measurement system which verifies the trajectory estimated by an IMU-based input device. For simple and robust implementation of the measurement system, a commercialized 6-DOF haptic device (PHANToM™) was used. To improve initialization, a mechanical jig and a software calibration algorithm were implemented. Experiments showed that this measurement setup provided a reference trajectory to verify the performance of the pen-type devices. Some of the remaining works are as follows: First, we will gather many data sets of handwriting trajectories from the pen-type device and the PHANToM™ device. These trajec-

tory data will be utilized to improve estimation algorithms for an optics-based trajectory, the inertia-based trajectory, and the error model compensated from an inertial sensor.

REFERENCES

[1] W. Walker, P. Lamere, P. Kwok, B. Raj, R. Singh, E. Gouvea, P. Wolf, and J. Woelfel, "Sphinx-4: A flexible open source framework for speech recognition," Sun Microsystems Laboratories November, 2004.

[2] T. E. Starner, B. Leibe, D. Minnen, T. Westyn, A. Hurst, and J. Weeks, The perceptive workbench: Computer-vision-based gesture tracking, object tracking, and 3D reconstruction for augmented desks, *Machine Vision and Applications*, 14, 59-71, (2003).

[3] Y. Fukuzaki, Position detecting apparatus and pointing device thereof Japan Patent, 3015275, 17 Dec., (1999).

[4] Y. Zloter and G. Shenholz, Infrared communications link with attachment configuration, US Patent, 6823105, Nov., 23, (2004).

[5] M. P. Petterssona and T. Edso, Coding pattern and apparatus and method for determining a value of at least one mark of a coding pattern, US Patent, 6663008, Dec., 16, (2003).

[6] H.-Y. Yang and S.-G. Lee, Pen type optical mouse device and method of controlling the same, US Patent, 7098894, Aug., 29, (2006).

[7] M. Epperson, Autonomous computer input device and marking instrument, US Patent, 5247137, Sep., 21, (1993).

[8] R. Gjone and J. Miraglia, "Pen for signature verification by acceleration and pressure," IBM Technical Disclosure BulletinJuly, 1981.

[9] W. Bang, W. Chang, K. Kang, E. Choi, A. Potanin, and D. Kim, Self-contained Spatial Input Device for Wearable Computers, in Proceedings of *The 7th IEEE International Symposium on Wearable Computers (ISWC'03)*, White Plains, NY, USA, pp.26-34, (2003).

[10] T. Miyagawa, Y. Yonezawa, K. Itoh, and M. Hashimoto, Handwritten pattern estimation using 3D inertial measurement of handwriting movement, *Trans. Society of Instrument and Control Engineers*, 38, Jan., (2002).

[11] S. J. Cho, J. K. Oh, W. C. Bang, W. Chang, E. S. Choi, Y. Jing, J. K. Cho, and D. Y. Kim, Magic Wand: A Hand-Drawn Gesture Input Device in 3-D Space with Inertial Sensors, *SAMSUNG Journal of Innovative Technology*, 1, 65-72, (2005).

[12] D. Titterton and J. Weston, *Strapdown Inertial Navigation Technology* 2nd ed.: IEE Press, (2004).

[13] T. H. Massie and J. K. Salisbury, The PHANTOM Haptic Interface: A Device for Probing Virtual Objects, in *Proceedings of the ASME Winter Annual Meeting, Symposium on Haptic Interfaces for Virtual Environment and Teleoperator Systems*, Chicago, IL, USA, (1994).

[14] J. J. Craig, *Introduction to Robotics*, 2nd ed. Reading, MA: Addison-Wesley Publishing Company, (1989).

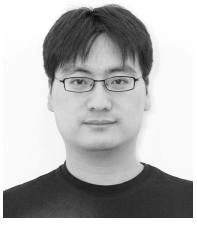

Seong Young Ko

He received a B.S. degree, an M.S. degree, and a Ph.D. degree in mechanical engineering from the Korea Advanced Institute of Science and Technology (KAIST), Daejeon, Korea, in 2000, 2002, and 2008, respectively. He was a visiting researcher in the Department of Electrical Engineering, University of Washington, USA for 6 months from 2005 to 2006. In 2008, he was a post-doctoral researcher in the Department of Electrical Engineering, KAIST, Korea, and from 2009, he is currently a research associate in the Mechatronics-In-Medicine Laboratory, the Department of Mechanical Engineering, Imperial College London, UK. His research interests include medical robotics, human-robot interaction and intelligent control.

Won-Chul Bang

He received a B.S. (1994) from Hanyang University, Korea and an M.S. (1996) and a Ph.D. (2001) from the Korea Advanced Institute of Science and Technology (KAIST) all in electrical engineering. From 2001 to 2002, he was a research associate at the Human-friendly Welfare Robot System Engineering Research Center. He currently works at Samsung Advanced Institute of Technology (SAIT) and is leading 3D Interaction and Intelligence part as a principal researcher. Dr. Bang first introduced the motion sensing/recognition technology into Samsung mobile phones. His research interests are motion sensing, gestural interaction, practical full-body motion tracking and haptic feedback.

Sang-Youn Kim

He received a B.S. (1994) from the Korea University, Korea and an M.S.E (1996) and a Ph.D. (2004) in mechanical engineering at Korea Advanced Institute of Science and Technology (KAIST). From 2004 to 2005, he was a researcher at the Human Welfare Robot System Research Center. In 2005, he was a research staff at Samsung Advanced Institute of Technology (SAIT). He is currently a professor of internet-media engineering at Korea University of Technology and Education. His current research interests include Haptics, Human-Computer Interaction, Virtual Reality, and Mobile Devices.